

Properties of strange hadronic matter in bulk and in finite systems

Jürgen Schaffner-Bielich

RIKEN BNL Research Center, Brookhaven National Laboratory, Upton, New York 11973

Avraham Gal

Racah Institute of Physics, The Hebrew University, Jerusalem 91904, Israel

(Received 23 May 2000; published 18 August 2000)

The hyperon-hyperon potentials due to a recent SU(3) Nijmegen soft-core potential model are incorporated within a relativistic mean field calculation of strange hadronic matter. We find considerably higher binding energy in bulk matter compared to several recent calculations which constrain the composition of matter. For small strangeness fractions ($f_S \lesssim 1$), matter is dominated by $N\Lambda\Xi$ composition and the calculated binding energy closely follows that calculated by using the hyperon potentials of our previous calculations. For larger strangeness fractions ($f_S \gtrsim 1$), the calculated binding energy increases substantially beyond any previous calculation due to a phase transition into $N\Sigma\Xi$ dominated matter. We also compare bulk matter calculations with finite system calculations, again highlighting the consequences of reducing the Coulomb destabilizing effects in finite strange systems.

PACS number(s): 21.80.+a, 13.75.Ev, 21.30.Fe, 21.90.+f

I. INTRODUCTION

Bodmer and Witten independently highlighted the idea that strange quark matter, with roughly equal composition of u , d , and s quarks leading to a strangeness fraction $f_S = -S/A \approx 1$ and a charge fraction $f_Q = Z/A \approx 0$, might provide the absolutely stable form of matter [1,2]. Metastable strange quark matter has been studied by Chin and Kerman [3]. Jaffe and collaborators [4,5] subsequently charted the various scenarios possible for the stability of strange quark matter, from absolute stability down to metastability due to weak decays. Finite strange quark systems, so called strangelets, have also been considered [4,6]. For a recent review of theoretical studies and experimental searches for strangelets, see Refs. [7,8].

Less advertised, perhaps, is the observation made in our previous work [9,10] that metastable strange systems with similar properties, i.e., $f_S \sim 1$ and $f_Q \sim 0$, might also exist in the hadronic basis at moderate values of density, between two and three times nuclear matter density. These strange systems are made out of nucleons (N), lambda (Λ), and cascade (Ξ) hyperons. The metastability of these strange hadronic systems was established by extending relativistic mean field (RMF) calculations from ordinary nuclei ($f_S = 0$) to multistrange nuclei with $f_S \neq 0$. Although the detailed pattern of metastability, as well as the actual values of the binding energy, depend specifically on the partly unknown hyperon potentials assumed in dense matter, the predicted phenomenon of metastability turned out to be robust in these calculations [10,11].

Quite recently, Stoks and Lee [12] have challenged the generality of the above results for strange hadronic systems. These authors constructed G matrices for coupled baryon-baryon channels, using an SU(3) extension [13] of the Nijmegen soft-core NSC97 potentials [14] from the $S=0$, -1 sector (to which data these potentials have been fitted) into the unexplored $S=-2, -3, -4$ sector. These G matrices were then employed within a Brueckner-Hartree-Fock (BHF)

calculation of strange hadronic matter (SHM) in bulk. The results showed that $N\Lambda\Xi$ systems are only loosely bound, and that charge-neutral strangeness-rich hadronic systems are unlikely to exist in nature in metastable form, in stark contrast to our earlier findings [9,10].

This vast difference in the predictions for the metastability and binding of SHM between following a BHF methodology, which uses an SU(3) extrapolated form of the NSC97 baryon-baryon potentials, and following a RMF methodology, which is based on mean fields designed to mimic the consequences of the Nijmegen hard-core potential model D [15], has prompted us to investigate possible origins of it. In this work we present calculational evidence for the incompleteness of the procedure applied by Stoks and Lee [12]. We do so by reproducing qualitatively their results for the instability and weak binding of $N\Lambda\Xi$ matter in bulk, within a *constrained* RMF calculation in which the mean fields are now designed to mimic the consequences of the NSC97 model used by Stoks and Lee. The constraints imposed by us, as a check, are identical with those imposed by these authors for the composition of SHM (see Fig. 4 of Ref. [12]). We argue that this is not the right way to identify minimum-energy equilibrium configurations for SHM. Indeed, doing the *unconstrained* RMF calculation with the same NSC97-inspired mean fields, we find qualitatively good agreement, for $f_S \lesssim 1$ where the bulk matter is $N\Lambda\Xi$ dominated, between these new results and our old results in model 2 [10]. For $f_S \gtrsim 1$, the new unconstrained calculation results in considerably higher binding energies than ever calculated for SHM, due to a phase transition into $N\Sigma\Xi$ dominated matter.

The paper is organized as follows. In Sec. II we describe the methodology of finding equilibrium configurations within the RMF formalism, and the input mean fields entering the new RMF calculations. Section III includes the results of these new calculations for *bulk* SHM, as well as for *finite* multistrange systems for which BHF calculations have not been done to date. The role of the Coulomb interaction in stabilizing charge-neutral strange systems is highlighted. Our

results are summarized and discussed in Sec. IV, where we also comment on the applicability of the SU(3)-extended NSC97 potential.

II. METHODOLOGY AND INPUT

We adopt the relativistic mean field model to describe strange hadronic matter in bulk and for finite systems of nucleons and hyperons. The model is an effective model where the parameters are adjusted to the known properties of nuclei and hypernuclei. We include in our extended RMF model all the $1/2^+$ baryons of the lowest SU(3) flavor octet, as well as hidden-strangeness meson exchange to allow for possibly strong hyperon-hyperon (YY) interactions. Here we use model 1 and model 2 of Ref. [9]. The basic ingredients of these models are the octet baryons matrix B , the matrices $V_\mu^{(8)}$ and $V_\mu^{(1)}$ of the vector meson octet and singlet, respectively, and the two scalar mesons σ and σ^* . In addition, a Coulomb term is included in finite system calculations. The Lagrangian is given as

$$\begin{aligned} \mathcal{L} = & \text{Tr} \bar{B} (i \gamma^\mu \partial_\mu - g_{\sigma B} \sigma - g_{\sigma^* B} \sigma^* - m_B) B - \frac{1}{2} (\partial^\mu \sigma \partial_\mu \sigma \\ & - m_\sigma^2 \sigma^2) - \frac{b}{3} \sigma^3 - \frac{c}{4} \sigma^4 - \frac{1}{2} (\partial_\nu \sigma^* \partial^\nu \sigma^* - m_{\sigma^*}^2 \sigma^{*2}) \\ & - g_v^{(8)} (\alpha \text{Tr} \bar{B} \gamma^\mu [V_\mu^{(8)}, B] + (1 - \alpha) \text{Tr} \bar{B} \gamma^\mu \{V_\mu^{(8)}, B\}) \\ & - g_v^{(1)} \text{Tr} \bar{B} \gamma^\mu B \cdot \text{Tr} V_\mu^{(1)} - \frac{1}{4} \text{Tr} V_{\mu\nu}^\dagger V^{\mu\nu} + \frac{1}{2} \text{Tr} m_v^2 V_\mu^\dagger V^\mu \\ & + \frac{1}{4} d (\omega_\mu \omega^\mu)^2. \end{aligned} \quad (1)$$

Here, both scalar fields are treated as singlets. The octet vector fields can be coupled in two ways, either antisymmetric (F type with $\alpha=1$) or symmetric (D type with $\alpha=0$). In the mean-field approximation, only the ω , ρ , and ϕ vector mesons remain operative. Their coupling constants to the baryon fields can be related by SU(3) symmetry [16]. By assuming ideal mixing of the vector mesons (i.e., the ϕ is a purely $s\bar{s}$ state), pure F -type coupling ($\alpha=1$), and that the nucleon does not couple to the ϕ , one recovers the SU(6) relations of the simple quark model

$$\begin{aligned} \frac{1}{3} g_{\omega N} &= \frac{1}{2} g_{\omega \Lambda} = \frac{1}{2} g_{\omega \Sigma} = g_{\omega \Xi}, \\ g_{\rho N} &= \frac{1}{2} g_{\rho \Sigma} = g_{\rho \Xi}, \quad g_{\rho \Lambda} = 0, \\ 2g_{\phi \Lambda} &= 2g_{\phi \Sigma} = g_{\phi \Xi} = -\frac{2\sqrt{2}}{3} g_{\omega N}, \quad g_{\phi N} = 0. \end{aligned} \quad (2)$$

Here, the constraint $3g_{\rho N} = g_{\omega N}$ is relaxed to allow the isovector coupling constant to be fixed by the isospin dependence of nuclear binding energies. The quark model is not

used for the scalar coupling constants, rather they are determined by adjusting to nuclear and hypernuclear properties. Self-interaction terms for the scalar field σ and the vector field ω are also included in the model. In the following, we use the parameter set TM1 of Ref. [17] where the parameters were taken from a fit to properties of spherical nuclei. The remaining scalar σ coupling constants for the hyperons are chosen to give reasonable hyperon potentials in saturated nuclear matter:

$$U_\Lambda^{(N)}(\rho_0) = -30 \text{ MeV},$$

$$U_\Sigma^{(N)}(\rho_0) = +30 \text{ MeV}, \text{ and } U_\Xi^{(N)}(\rho_0) = -18 \text{ MeV}. \quad (3)$$

Note, that these relativistic potentials are (10–20)% stronger than the corresponding nonrelativistic values. The values for Σ and Ξ hyperons differ from the previous choice of Refs. [9,10], reflecting recent developments in hypernuclear physics which are briefly recorded below.

For the Σ nuclear interaction, the most updated analysis of Σ^- atomic data indicates a repulsive isoscalar potential in the interior of nuclei [18] which is compatible with the absence of bound-state or continuum peaks in a recent search for Σ hypernuclei [19]. In fact, the only Σ hypernuclear bound state found so far is $^4_\Sigma\text{He}$ [20,21], where the binding results from the strong isovector component of the Σ nuclear interaction. These statements are supported by several recent calculations [22,23]. The precise magnitude of the depth of the Σ nuclear potential is of little importance to our investigations. It turns out that the Σ hyperon will not appear anyway in the bulk matter calculation, or in the finite system calculations within models 1 and 2, unless its hadronic interactions are exceptionally strong, so as to block the release of about 75 MeV in the free-space $\Sigma B \rightarrow \Lambda B$ strong-interaction conversion.

For the Ξ nuclear interaction, measurements of the final-state interaction of Ξ hyperons produced in the (K^-, K^+) reaction on ^{12}C in experiments E224 at KEK [24] and E885 at the AGS [25] indicate a nonrelativistic potential $U_{\Xi, \text{nr}}^{(N)}$ of about -16 and -14 MeV or less, respectively. Below we will actually vary the value for $U_{\Xi}^{(N)}$ to check its effect on the binding energy of SHM.

The hyperon (Y) potentials $U_Y^{(Y')}$ in hyperon (Y') matter, in the absence of direct experimental data, depend to a large extent on the assumptions made on the underlying YY interactions. In model 1, which does not use σ^* and ϕ exchanges, the potentials $U_Y^{(Y')}$ are rather weak, less than 10 MeV deep. The exchange of these hidden-strangeness mesons is included in model 2, where the σ^* coupling to hyperons is adjusted so that the potential of a single hyperon, embedded in a bath of Ξ matter at nuclear saturation density ρ_0 , becomes

$$U_{\Xi}^{(\Xi)}(\rho_0) = U_{\Lambda}^{(\Xi)}(\rho_0) = -40 \text{ MeV}, \quad (4)$$

in accordance with the attractive YY interactions of the Nijmegen potential model D [10]. The resulting $U_{\Lambda}^{(\Lambda)}$ is about -20 MeV, considerably more attractive than in model 1. Indeed the few double Λ hypernuclear events observed so far in emulsion require a relatively strong $\Lambda\Lambda$ attractive in-

teraction [26], which lends support to model 2 over model 1, but the actual situation for the other, unknown, YY' channels could prove more complex than allowed for by either model. All that may be said at present is that, as far as the $\Lambda\Lambda$ interaction strength is concerned, model 2 is a more realistic one than model 1.

Since there appears some confusion in the recent literature [12,27] regarding how to calculate self-consistently the properties of SHM in bulk, we will ponder on the thermodynamically consistent methodology in more detail. As we will demonstrate in the following, a major property of SHM within the SU(3)-extended NSC97 model might have been overlooked in these works. Here we focus on the thermodynamically correct treatment in the RMF approximation. The extension to BHF calculations is then straightforward. Very recently, thermodynamically consistent BHF calculations of β -stable strange matter in neutron stars have been performed by Baldo *et al.* [28], using the NSC89 model [29] for the YN interactions, and by Vidaña *et al.* [30], using the SU(3)-extended NSC97 model [13] for the YN and YY interactions.

In general, we can describe the system by the grand-canonical thermodynamic potential Ω , which depends on the temperature T , the volume V , and the independently conserved chemical potentials μ_α . At $T=0$, the pressure is given by

$$P(\mu_\alpha) = -\Omega(\mu_\alpha, T=0)/V. \quad (5)$$

For SHM in bulk, since the isospin dependence is usually suppressed, there are just two conserved charges in bulk which are the baryon number B and the strangeness number S . The chemical potentials of the individual baryons can be related to the corresponding baryon chemical potential μ_B and strangeness chemical potential μ_S by

$$\mu_i = B_i \cdot \mu_B + S_i \cdot \mu_S. \quad (6)$$

This ensures that the system is in chemical equilibrium or, in other words, that the strangeness and baryon numbers are conserved in all possible strong-interaction reactions in the medium, such as

$$\Sigma + N \leftrightarrow \Lambda + N, \quad \Lambda + \Lambda \leftrightarrow \Xi + N, \quad \Lambda + \Xi \leftrightarrow \Sigma + \Xi, \dots \quad (7)$$

The Hugenholtz–van Hove theorem relates the Fermi energy of each baryon to its chemical potential in equilibrated matter

$$\mu_i = E_{F,i} = \sqrt{k_{F,i}^2 + m_i^{*2}} + g_{\omega i} \omega_0 + g_{\rho i} \rho_0 + g_{\phi i} \phi_0. \quad (8)$$

Here we used the energy-momentum relation of the mean-field approximation with the effective mass $m_i^* = m_i + g_{\sigma i} \sigma + g_{\sigma^* i} \sigma^*$ for the baryon species i . Note, that these potentials depend on the overall composition of the matter, requiring thus a self-consistent calculation. Equation (8) can be easily solved to calculate the Fermi momenta $k_{F,i}$ and hence the number density of baryon i for given chemical potentials

$$\rho_i = \gamma_i \frac{k_{F,i}^3}{6\pi^2}, \quad (9)$$

where γ_i is the spin-isospin degeneracy factor. If the solution results in an imaginary Fermi momentum, the particle is not present in the system and the corresponding density is set to zero. In Brueckner theory, one has to solve for an equation of the form

$$\mu_i = E_i(k_{F,i}) = m_i + \frac{k_{F,i}^2}{2m_i} + \text{Re } U_i(k_{F,i}) \quad (10)$$

since the potential is now momentum dependent. It is apparent from the above procedure that no baryon species may be ignored *a priori*, but one has to check for their appearance by calculating the corresponding Fermi momentum. Therefore, any calculation of baryonic matter with nucleons and Λ 's alone is bound to violate the condition of chemical equilibrium Eq. (6), since Σ and particularly Ξ hyperons are likely to appear in strange hadronic systems [11]. In that sense, multi- Λ matter calculations as performed in Refs. [31–37] are incomplete. Furthermore, the Fermi momenta of different baryon species cannot be set equal to each other, since this again violates the condition of chemical equilibrium. If one arbitrarily sets certain baryon fractions to be equal to each other, as, e.g., done in, Ref. [12], the resulting system is not in its energetically favored global minimum and the computed binding energies will be underestimated. In addition, the overall pressure of the system will be too low, resulting in a too soft equation of state; maximum masses of neutron stars computed in this way will be underestimated.

The pressure and the energy density in the RMF model in bulk are given by

$$\begin{aligned} P = & -\frac{1}{2} m_\sigma^2 \sigma^2 - \frac{b}{3} \sigma^3 - \frac{c}{4} \sigma^4 - \frac{1}{2} m_{\sigma^*}^2 \sigma^{*2} + \frac{1}{2} m_\omega^2 \omega_0^2 \\ & + \frac{1}{4} d \omega_0^4 + \frac{1}{2} m_\phi^2 \phi_0^2 + \sum_{i=B,l} \frac{\gamma_i}{(2\pi)^3} \int_0^{k_{F,i}} d^3 k \frac{k^2}{\sqrt{k^2 + m_i^{*2}}, \\ \epsilon = & \frac{1}{2} m_\sigma^2 \sigma^2 + \frac{b}{3} \sigma^3 + \frac{c}{4} \sigma^4 + \frac{1}{2} m_{\sigma^*}^2 \sigma^{*2} + \frac{1}{2} m_\omega^2 \omega_0^2 + \frac{3}{4} d \omega_0^4 \\ & + \frac{1}{2} m_\phi^2 \phi_0^2 + \sum_{i=B,l} \frac{\gamma_i}{(2\pi)^3} \int_0^{k_{F,i}} d^3 k \sqrt{k^2 + m_i^{*2}}, \quad (11) \end{aligned}$$

respectively. The binding energy per baryon is then obtained by subtracting the properly weighted combination of the rest masses from the energy density of the system

$$E/A = \frac{1}{\rho_B} (\epsilon - \rho_N \cdot m_N - \rho_\Lambda \cdot m_\Lambda - \rho_\Sigma \cdot m_\Sigma - \rho_\Xi \cdot m_\Xi). \quad (12)$$

The meson fields are determined by their equations of motion (see, e.g., Ref. [38]). The particle densities are calculated using the thermodynamically consistent formalism as outlined above.

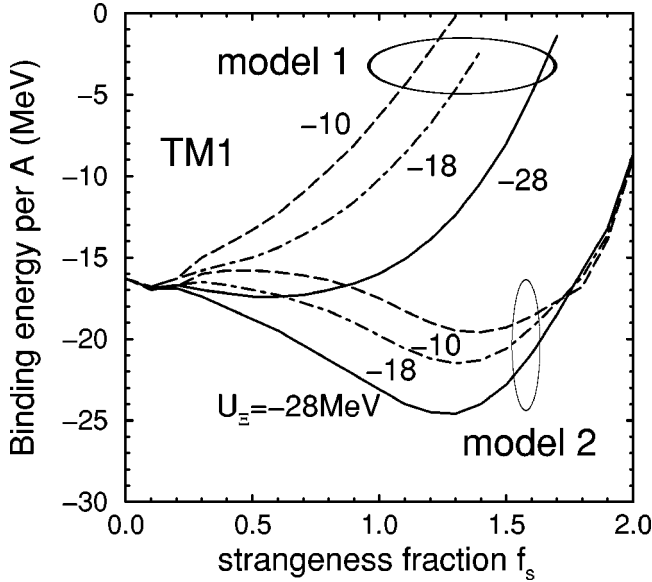


FIG. 1. Binding energy per baryon of SHM in models 1 and 2, with different choices of the Ξ potential in nuclear matter.

For most purposes, one wishes to translate the dependence on the two chemical potentials into their corresponding baryon and strangeness number density. This is done using the expressions for overall baryon and strangeness number conservation

$$\rho_B = \sum_i B_i \cdot \rho_{V,i} = \rho_N + \rho_\Lambda + \rho_\Sigma + \rho_\Xi, \quad (13a)$$

$$\rho_S = \sum_i (-S_i) \cdot \rho_{V,i} = \rho_\Lambda + \rho_\Sigma + 2\rho_\Xi, \quad (13b)$$

where $\rho_{V,i}$ is the vector density of baryon species i . A useful measure of the strangeness contents of the system is given by the strangeness fraction

$$f_S = \frac{\rho_S}{\rho_B} = \frac{\rho_\Lambda + \rho_\Sigma + 2\rho_\Xi}{\rho_N + \rho_\Lambda + \rho_\Sigma + \rho_\Xi}. \quad (14)$$

III. RESULTS

Plots of calculated binding energy of SHM per baryon as function of the strangeness fraction f_S are shown in Fig. 1, for different choices of the Ξ nuclear potential denoted by U_Ξ , in models 1 and 2 [9,10]. For $f_S=0$, there are only nucleons in the system and one gets the standard equation of state of nuclear matter as function of baryon density. The equilibrium density of nuclear matter is determined by minimizing the binding energy with respect to the baryon density. The resulting minimum value of binding energy per nucleon is shown then at $f_S=0$ in the plots of Fig. 1. Next, we increase the strangeness fraction from zero on, and the system of equations adjusts itself at each fixed value of f_S to find the corresponding baryon densities ensuring chemical equilibrium [Eq. (6)]. The minimum value of the binding energy per baryon as function of baryon density at each fixed strange-

ness fraction is then plotted in Fig. 1 for the corresponding value of f_S . In this way, one gets the binding energy of SHM as function of the strangeness fraction. It turns out that Σ hyperons do not appear at any value of f_S in both models 1 and 2. To display the dependence on the Ξ nuclear potential we chose three different values, $U_\Xi = -10, -18, -28$ MeV. The variation in the plots of model 1 is quite pronounced. For $U_\Xi = -28$ MeV, the minimum is at a finite value $f_S=0.6$, with a binding energy per baryon of -17.4 MeV. For shallower Ξ potentials, this minimum disappears and slightly strange matter with $f_S \approx 0.1$ is the most strongly bound configuration. On the other hand, in model 2, varying U_Ξ does not lead to drastic changes. The minimum in the binding energy per baryon for $U_\Xi = -28$ MeV, at $f_S=1.3$ with $E/A = -24.6$ MeV, is shifted to $E/A = -21.5$ MeV for $U_\Xi = -18$ MeV and to $E/A = -19.6$ MeV at a slightly higher value $f_S=1.4$ for $U_\Xi = -10$ MeV. The reason is that in model 2 the minimum is generated by the YY interactions which have been adjusted according to Eq. (4), so that the binding energy curves in model 2 are not as much affected by changing U_Ξ as compared to the effect of this change in model 1. Note that the constraint (4) ensures that pure Ξ matter ($f_S=2$) has the same binding energy, $E/A = -8.9$ MeV, in all three cases. Pure Ξ matter is always unbound in model 1 due to the missing attraction in the YY channels.

Substantial departures from the universality [Eq. (4)] assumed in Refs. [9,10] for the YY interactions occur in the most recent SU(3) extension of the Nijmegen soft-core potential model NSC97 [13]. In particular, the $\Sigma\Sigma$ and $\Xi\Xi$ interactions are predicted to be highly attractive in some channels, leading to bound states. We wish to examine the consequences of this model in our RMF calculation of SHM. The YY interactions of Ref. [13] are implemented in our calculation by adjusting the coupling constants of the σ^* meson field to reproduce qualitatively the hyperon binding energy curves shown in Fig. 2 of Ref. [12] for set NSC97f. All the other coupling constants are held fixed, so that we still get the hyperon potentials of Eq. (3) in nuclear matter. The resulting binding energy curves, of each baryon species j in its own matter $B_j^{(j)}$, are depicted in Fig. 2 as function of density. For nucleons, we again use the parametrization TM1 so as to get the correct binding energy at the correct saturation density ρ_0 . Note that NSC97f does not reproduce the correct nuclear matter saturation point, but gives a too shallow minimum at a too high density (see Fig. 2 of Ref. [12]). No binding occurs for Λ hyperons, and $B_\Lambda^{(\Lambda)}$ reaches $+20$ MeV already at rather low density, $\rho=0.1 \text{ fm}^{-3}$. This strong repulsive ‘‘potential’’ is due to the very weak underlying $\Lambda\Lambda$ interaction in the extended NSC97f model which is incompatible with the fairly strong $\Lambda\Lambda$ attraction necessary to explain the observed double Λ hypernuclear events (see Refs. [26,39], and references therein). On the other hand, Σ matter is deeply bound, by -33 MeV per baryon at $\rho=0.58 \text{ fm}^{-3}$ which is twice as deep as ordinary nuclear matter, and Ξ matter has a binding energy of -23 MeV per baryon at $\rho=0.39 \text{ fm}^{-3}$. It is clear from Fig. 2 that a mixture of Σ and Ξ matter must be very deeply bound too, unless there is an overwhelmingly repulsive interaction be-

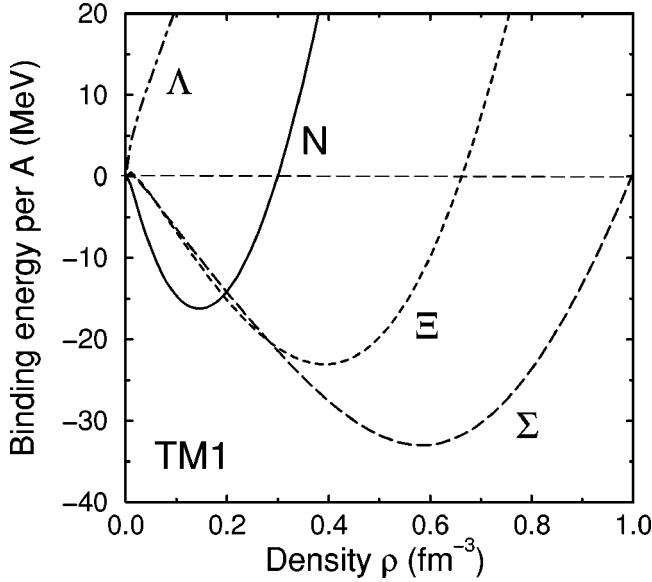


FIG. 2. Binding energy per nucleon (N) in nucleon matter, compared to the binding energy per hyperon (Λ, Σ, Ξ) in its own hyperonic matter. The hyperonic parameters were chosen to reproduce the binding energy minima of Fig. 2 in Ref. [12].

tween Σ and Ξ hyperons. Actually, the interaction between Σ and Ξ hyperons is the most attractive one in the extended NSC97f model, giving rise to the deepest bound $\Sigma\Xi$ dibaryon state [13]. Independently, increasing the number of degrees of freedom will also result in a more deeply bound state. This is the case, for example, when going from unbound neutron matter ($\gamma=2$) to bound nuclear matter ($\gamma=4$). Therefore, one expects that $\Sigma\Xi$ matter is in fact more deeply bound than Σ or Ξ matter alone. In the following, we will denote the parametrization responsible for the curves of Fig. 2 as model N .

Figure 3 shows the binding energy of SHM per baryon in model N as function of strangeness fraction. For comparison, the curves for models 1 and 2 from Fig. 1 are also plotted. We performed two different calculations for model N : one where the hyperon fractions $\chi_i = \rho_i / \rho_B$ are held equal by hand ($\chi_\Lambda = \chi_\Sigma = \chi_\Xi$) as done in Ref. [12], and the self-consistent one where the hyperon fractions are determined so as to ensure chemical equilibrium (denoted as ‘‘equil.’’ in the figure). It is evident from Fig. 3 that the self-consistent treatment gives a substantially lower energy, since it is the unconstrained minimum-energy solution. The disagreement between the results of the two calculations increases with f_S . At $f_S=1$ the difference between the two curves amounts to nearly 10 MeV. The curve for model N follows closely the one for model 2 up to a strangeness fraction of $f_S=0.95$. At larger values of f_S a deep minimum develops due to the highly attractive interaction between the Σ and Ξ hyperons. Note that an equal mixture of Σ 's and Ξ 's gives $f_S=1.5$ and the minimum of the curve is close to that point, i.e., $E/A = -79$ MeV at $f_S=1.45$. For larger values of f_S , the curve denoted by N rises again, ending up at $f_S=2$ with the same binding energy per hyperon as that shown in Fig. 2 for pure Ξ matter. The deep minimum around $f_S=1.5$ results from

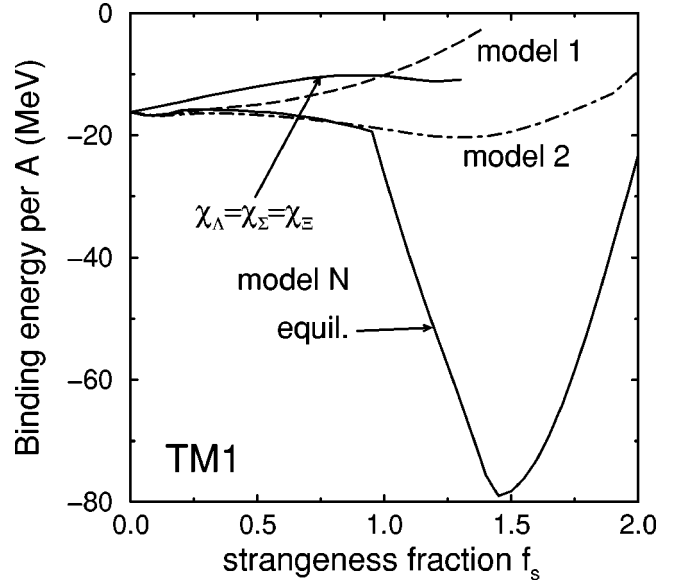


FIG. 3. Comparison of the binding energy of SHM per baryon in models 1 (dash), 2 (dash-dot), and N (solid). The upper solid line shows the result for the constrained case of equal hyperon fractions ($\chi_\Lambda = \chi_\Sigma = \chi_\Xi$), the lower one shows the curve for the correct, unconstrained equilibrium calculation.

the deep binding of Σ plus Ξ matter which is stronger than seen in Fig. 2 for matter composed of either one of these species separately. This deep minimum structure can only be reached when the hyperon fractions are allowed to adjust self-consistently. Fixing the hyperon fractions, as done in Ref. [12], will always give a curve which is higher in energy, risking the loss of some important features of the model. In fact, the curve for the constrained calculation [12] ends up at $f_S=4/3$ due to the particular constraint applied.

The deep minimum seen in Fig. 3 emerges due to a second minimum in the corresponding equation of state at high strangeness fraction, connected with a first order phase transition from matter consisting of $N\Lambda\Xi$ baryons to $N\Sigma\Xi$ baryonic matter. This transition is visualized in Fig. 4 where the binding energy is drawn versus the baryon density for several representative fixed values of f_S . For $f_S=0.8$, there is a global minimum at a baryon density of $\rho_B = 0.27$ fm^{-3} . A shallow local minimum is seen at larger baryon density at $\rho_B = 0.72$ fm^{-3} . Increasing the strangeness fraction to $f_S=0.9$ lowers substantially the local minimum by about 20 MeV, whereas the global minimum barely changes. At $f_S=1.0$ this trend is amplified and the relationship between the two minima is reversed, as the minimum at higher baryon density becomes energetically lower than the one at lower baryon density. The system will then undergo a transition from the low density state to the high density state. Due to the barrier between the two minima, it is a first-order phase transition from one minimum to the other.

Figure 5 demonstrates explicitly that the phase transition involves transformation from $N\Lambda\Xi$ dominated matter to $N\Sigma\Xi$ dominated matter, by showing the calculated composition of SHM for model N as function of the strangeness fraction f_S . The particle fractions χ_i for each baryon species change as function of f_S . At $f_S=0$, one has pure nuclear

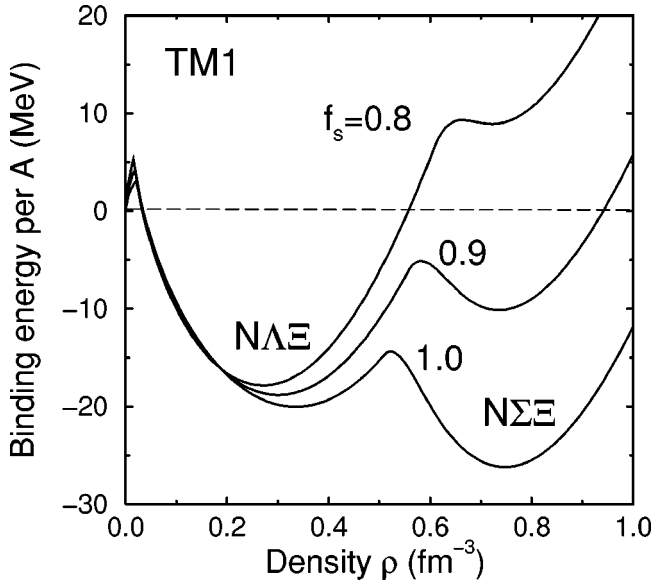


FIG. 4. Transition from $N\Lambda\Xi$ matter to $N\Sigma\Xi$ matter in model N . A second minimum appears at higher density for a strangeness fraction of $f_s=0.8$, becoming more stable for higher strangeness fraction ($f_s=1$).

matter, whereas at $f_s=2$ one has pure Ξ matter. In between, matter is composed of baryons as dictated by chemical equilibrium. A change in the particle fraction may occur quite drastically when new particles appear, or existing ones disappear in the medium. A sudden change in the composition is seen in Fig. 5 for $f_s=0.2$ when Ξ 's emerge in the medium, or at $f_s=1.45$ when nucleons disappear. The situation at $f_s=0.95$ is a special one, as Σ 's appear in the medium, marking the first-order phase transition observed in the previous figure. The baryon composition alters completely at that point, from $N\Xi$ baryons plus a rapidly vanishing frac-

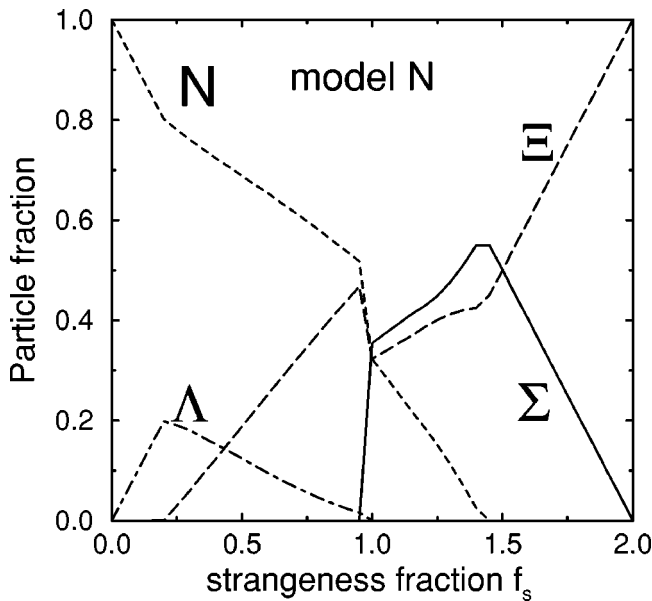


FIG. 5. Composition of SHM in model N versus the strangeness fraction. Σ hyperons appear around $f_s=1$.

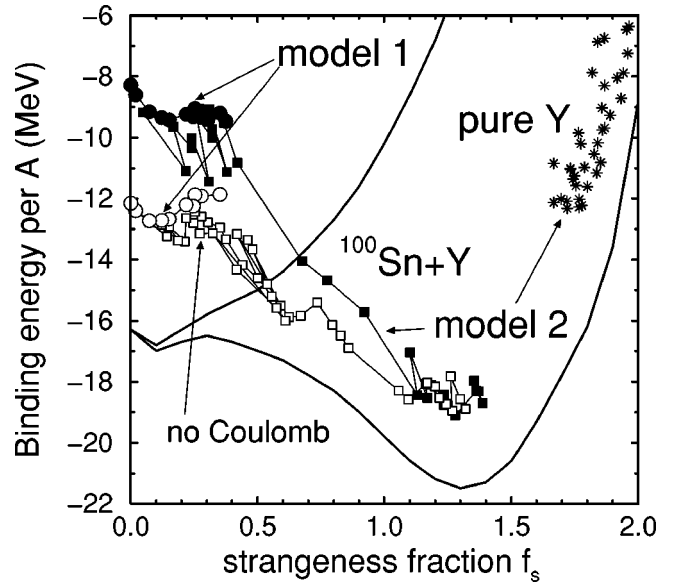


FIG. 6. Binding energy of multi-strange finite systems built on a ^{100}Sn nuclear core in models 1 (circles) and 2 (squares, stars), with and without Coulomb effects. The curves for bulk SHM (solid lines) are also shown.

tion of Λ 's into $\Sigma\Xi$ hyperons plus a decreasing fraction of nucleons. At the minimum of the binding energy curve in Fig. 3, the matter is composed mainly of Σ 's and Ξ 's with a very small admixture of nucleons.

Last but not least, we discuss *finite* systems of SHM for which the Coulomb interaction plays a significant role. We also performed calculations switching off the Coulomb interaction in order to study separately the effects due to the possibly strong YY interactions. Yet, we will not pursue for finite systems the implications of the deep minimum found in model N , but rather stick in the following to the more conservative models 1 and 2. Our choice for the Ξ potential is $U_{\Xi} = -18$ MeV, in accordance with the recent observations [24,25]. Following the procedure outlined in Refs. [9,10] we start from a ‘‘normal’’ nucleus (here ^{100}Sn , for example) and add Λ hyperons to the system. As soon as the strong decay reactions $p\Xi^- \rightarrow \Lambda\Lambda$ or $n\Xi^0 \rightarrow \Lambda\Lambda$ are Pauli-blocked, we start adding Ξ hyperons. For each given system of nucleons and hyperons, we check that the two reactions are blocked also in reverse, so that the whole multi-strange nucleus is metastable, decaying only via weak interactions. These calculations also include the effects of the ρ meson field, in order to properly account for symmetry-energy contributions to the binding energy.

Our results are summarized in Fig. 6. The solid lines are the binding energy curves for SHM in bulk for model 1 (upper curve) and model 2 (lower curve), taken from Fig. 1 for the value $U_{\Xi} = -18$ MeV. The filled symbols denote systems where the Coulomb interaction is included, the open symbols stand for the case where the Coulomb interaction has been switched off. For model 1, shown in circles, SHM is slightly more bound than the core nucleus ^{100}Sn . For the highest strangeness fraction we found, $f_s=0.375$, the system is bound by $E/A = -9.5$ MeV, compared to $E/A = -8.3$

MeV for ^{100}Sn . When the Coulomb interaction is turned off, the curve shifts down by several MeV per baryon. The chargeless core nucleus ^{100}Sn is then bound by $E/A = -12.2$ MeV, whereas the strangeness richest object has now a slightly lower binding energy per baryon of $E/A = -11.9$ MeV. Hence, the main effect for the increased binding energy of SHM in model 1 actually comes from Coulomb effects. The negatively charged Ξ^- hyperons neutralize the positively charged protons, making SHM more bound than ordinary nuclei. Still, the binding energies found are well above the curve for bulk matter due to finite size effects, such as surface tension.

The situation is different in model 2, for which results are shown by squares in Fig. 6. Due to the attractive YY interactions in this model, the binding energy per baryon increases substantially to a value of $E/A = -19$ MeV at $f_S = 1.3$, which is even deeper than the binding energy of nuclear matter in bulk. This high value of binding is obtained irrespective of whether or not the Coulomb interaction is included, since for such high values of strangeness fraction the total charge fraction of the system is close to zero. Obviously, in model 2 the tremendously increased binding energy of SHM originates mostly from the attractive YY interactions, and only to a minor extent from the reduced Coulomb repulsion. Note that the binding energy for the deepest lying systems in model 2 is close to the values for SHM in bulk matter which are shown by the lower solid line. These systems are quite heavy, with mass numbers of about $A = 400$ and higher, so that finite size effects become quite small.

In addition, we also plotted the binding energies of purely hyperonic systems which consist of $\Lambda \Xi^0 \Xi^-$ hyperons solely and, therefore, do not need to be Pauli blocked in order to keep them metastable [9,10]. Since these systems can decay only via weak interaction, arbitrary numbers for the three different hyperon species are allowed. We find that purely hyperonic objects are bound up to $E/A = -12$ MeV per hyperon. The binding energies, denoted by stars in the figure, follow the trend of the bulk calculation curve (solid line).

IV. SUMMARY AND CONCLUSIONS

In the present work we have calculated the minimum-energy equilibrium composition of bulk SHM made out of the SU(3) octet baryons N , Λ , Σ , and Ξ , over the entire range of strangeness fraction $0 \leq f_S \leq 2$, for meson fields which generate, within the RMF model, qualitatively similar baryon potentials to those generated from the SU(3) extension of the NSC97 potential model [13] using the BHF approximation [12]. Our main results are displayed in Fig. 3 which shows that SHM is comfortably metastable in this model N for any allowed value of $f_S > 0$. The $N\Lambda\Xi$ composition and the binding energy calculated for equilibrium configurations with $f_S \leq 1$ resemble those of model 2 in our earlier work [9,10]. The use of models 2 and N [10,13] implies sizable YY attractive interactions which differ, however, in detail between the two models. The model of Ref. [13] yields particularly attractive $\Xi\Xi$, $\Sigma\Sigma$, and $\Sigma\Xi$ interactions, but vanishingly weak $\Lambda\Lambda$ and $N\Xi$ interactions. We remark that

this extent of weakness is in fact ruled out by the little information one has from $\Lambda\Lambda$ hypernuclei [26] and from Ξ -nucleus interactions [24,25]. On the other hand, model 2 of Ref. [10] accounts more realistically for the attractive $\Lambda\Lambda$ and $N\Xi$ interactions, but ignores altogether Σ hyperons which require exceptionally strong binding in order to overcome the strong interaction $\Sigma B \rightarrow \Lambda B$ conversion which in free space releases about 75 MeV. Yet, all these differences between the two models regarding the relative size of interactions within $N\Lambda\Xi$ dominated matter hardly matter when it comes to establishing the stability and binding pattern of this multistrange matter. In this sense, SHM is a robust phenomenon. The metastability of SHM has also been recently confirmed within the modified quark-meson coupling model [40].

The difference between models 2 and N clearly shows up for $f_S \geq 1$, where Σ 's replace Λ 's in model N due to their exceptionally strong attraction to Σ and Ξ hyperons. Figures 3, 4, and 5 of the present work give evidence for a phase transition, from $N\Lambda\Xi$ dominated matter for $f_S \leq 1$ to $N\Sigma\Xi$ dominated matter for $f_S \geq 1$, with binding energies per baryon reaching as much as 80 MeV. This effect has gone unnoticed in previous works which by constraining the composition of matter in bulk did not allow for the most general minimum-energy equilibrium configurations. In contrast, our model 2 produces a much smoother pattern of binding over the entire range of f_S , with a gain of only approximately 5 MeV per baryon (at $f_S \approx 1.3$) for the bulk matter calculation. However, for *finite* multistrange systems the gain can be considerably bigger, due to getting rid of most of the Coulomb repulsion for such approximately charge-neutral systems, amounting to almost 11 MeV per baryon for the examples of Fig. 6.

We checked also for the critical strength of the Ξ -nuclear potential below which finite systems of SHM would consist only of nucleons and Λ hyperons in model 1. Of course, the critical value for U_Ξ depends on the size of the system. For a nuclear core of ^{16}O with 8 Λ 's filling up the s and p shells, Ξ 's cannot be added to the system for a potential shallower than $U_\Xi^c = -13$ MeV. In the case of ^{56}Ni , this critical value shifts to $U_\Xi^c = -10$ MeV. For the ^{100}Sn nuclear core used to demonstrate finite systems of SHM in our present calculation (see Fig. 6), we find a critical strength $U_\Xi^c = -7$ MeV for which the $\Xi N \rightarrow \Lambda\Lambda$ strong-interaction conversion is barely Pauli blocked. However, U_Ξ needs to become more attractive than the above critical values demonstrate, in order that the corresponding multistrange finite systems also remain *particle stable*. We remind the reader that the value $U_\Xi = -18$ MeV used in the figure was designed to agree with the present phenomenological estimates [24,25]. In bulk matter, Ξ -nucleus potentials as repulsive as $U_\Xi = +40$ MeV still admit bound Ξ 's just before SHM gets unbound at $f_S = 0.7$. The reason for this behavior is that the constraint $f_S = 0.7$ introduces Ξ 's in matter even though their interaction is repulsive. The Fermi momentum of the Λ 's become sufficiently high so that it pays to create some seemingly unfavorable Ξ 's in order to lower the Λ Fermi momentum. Note that SHM in model 2 always contains Ξ 's, irrespective of the

nature of U_{Ξ} , by virtue of the attractive underlying YY interactions.

While it is true that the RMF model 2 is a schematic model and is linked only indirectly to the underlying baryon-baryon interactions, it is nevertheless constrained by Λ and Ξ nuclear phenomenology, and by the few $\Lambda\Lambda$ hypernuclear species reported to date. The extrapolation to YY channels which underlie the hyperon potentials in hyperon matter is more conservative in this model than in model N inspired by the SU(3) extension of the NSC97 potential model [13]. We emphasize that although the NSC97 model [14] has been tuned up to reproduce certain characteristics of Λ hypernuclei, particularly its version NSC97f, the predictions elsewhere of these models appear invariably ruled out by whatever experimental hints one has to date. In addition to the exceedingly weak $\Lambda\Lambda$ and $N\Xi$ interactions already mentioned above, the NSC97 model overbinds Λ hyperons in nuclear matter ($U_{\Lambda} \sim -38$ MeV) and gives rise to quite attractive Σ nuclear potential ($U_{\Sigma} \sim -20$ MeV) in BHF calculations [27], whereas the phenomenology of Σ^{-} atoms [18] and ‘‘hypernuclei’’ [22] indicates a much weaker, if not a

repulsive, Σ nuclear potential. Furthermore, the NSC97 model gives rise to a sizable Σ nuclear symmetry energy which is opposite in sign [27] to that of the earlier NSC89 model [29] and, more importantly, to that established phenomenologically [18,22,23]. We therefore suggest that the consequences of the NSC97 model in dense SHM, as exemplified here, should be taken with a grain of salt. More dedicated work is required to amend the pitfalls of this model (for a recent discussion in this direction see Ref. [41]).

ACKNOWLEDGMENTS

J.S.B. thanks RIKEN, Brookhaven National Laboratory and the U.S. Department of Energy for providing the facilities essential for the completion of this work. The work of A.G. was supported in part by a DFG Trilateral Grant No. 243/51-2. A.G. also wishes to thank Larry McLerran, Sidney Kahana, and John Millener for their hospitality during a supported visit to the Nuclear Theory Group at the Brookhaven National Laboratory in February 2000.

-
- [1] A.R. Bodmer, Phys. Rev. D **4**, 1601 (1971).
 - [2] E. Witten, Phys. Rev. D **30**, 272 (1984).
 - [3] S.A. Chin and A.K. Kerman, Phys. Rev. Lett. **43**, 1292 (1979).
 - [4] E. Farhi and R.L. Jaffe, Phys. Rev. D **30**, 2379 (1984).
 - [5] M.S. Berger and R.L. Jaffe, Phys. Rev. C **35**, 213 (1987).
 - [6] E.P. Gilson and R.L. Jaffe, Phys. Rev. Lett. **71**, 332 (1993).
 - [7] J. Schaffner-Bielich, Nucl. Phys. **A639**, 443c (1998).
 - [8] J.L. Nagle for the E864 Collaboration, Nucl. Phys. **A661**, 185c (1999).
 - [9] J. Schaffner, C.B. Dover, A. Gal, C. Greiner, and H. Stöcker, Phys. Rev. Lett. **71**, 1328 (1993).
 - [10] J. Schaffner, C.B. Dover, A. Gal, D.J. Millener, C. Greiner, and H. Stöcker, Ann. Phys. (N.Y.) **235**, 35 (1994).
 - [11] S. Balberg, A. Gal, and J. Schaffner, Prog. Theor. Phys. Suppl. **117**, 325 (1994).
 - [12] V.G.J. Stoks and T.S.H. Lee, Phys. Rev. C **60**, 024006 (1999).
 - [13] V.G.J. Stoks and Th.A. Rijken, Phys. Rev. C **59**, 3009 (1999).
 - [14] Th.A. Rijken, V.G.J. Stoks, and Y. Yamamoto, Phys. Rev. C **59**, 21 (1999).
 - [15] M.M. Nagels, T.A. Rijken, and J.J. de Swart, Phys. Rev. D **15**, 2547 (1977).
 - [16] C.B. Dover and A. Gal, Prog. Part. Nucl. Phys. **12**, 171 (1984).
 - [17] Y. Sugahara and H. Toki, Nucl. Phys. **A579**, 557 (1994).
 - [18] J. Mareš, E. Friedman, A. Gal, and B.K. Jennings, Nucl. Phys. **A594**, 311 (1995).
 - [19] S. Bart *et al.*, Phys. Rev. Lett. **83**, 5238 (1999).
 - [20] R.S. Hayano *et al.*, Phys. Lett. B **231**, 355 (1989).
 - [21] T. Nagae *et al.*, Phys. Rev. Lett. **80**, 1605 (1998).
 - [22] J. Dabrowski, Phys. Rev. C **60**, 025205 (1999).
 - [23] T. Harada, Nucl. Phys. **A672**, 181 (2000).
 - [24] T. Fukuda *et al.*, Phys. Rev. C **58**, 1306 (1998).
 - [25] P. Khaustov *et al.*, Phys. Rev. C **61**, 054603 (2000).
 - [26] C.B. Dover, D.J. Millener, A. Gal, and D.H. Davis, Phys. Rev. C **44**, 1905 (1991).
 - [27] I. Vidaña, A. Polls, A. Ramos, M. Hjorth-Jensen, and V.G.J. Stoks, Phys. Rev. C **61**, 025802 (2000).
 - [28] M. Baldo, G.F. Burgio, and H.-J. Schulze, Phys. Rev. C **61**, 055801 (2000).
 - [29] P.M.M. Maessen, Th.A. Rijken, and J.J. de Swart, Phys. Rev. C **40**, 2226 (1989).
 - [30] I. Vidaña, A. Polls, A. Ramos, L. Engvik, and M. Hjorth-Jensen, nucl-th/0004031.
 - [31] K. Ikeda, H. Bando, and T. Motoba, Prog. Theor. Phys. **81**, 147 (1985).
 - [32] J. Mareš and J. Žofka, Z. Phys. A **333**, 209 (1989); **345**, 47 (1993).
 - [33] M. Rufa, J. Schaffner, J. Maruhn, H. Stöcker, W. Greiner, and P.G. Reinhard, Phys. Rev. C **42**, 2469 (1990).
 - [34] M. Barranco, R.J. Lombard, S. Marcos, and S.A. Moszkowski, Phys. Rev. C **44**, 178 (1991).
 - [35] D.E. Lanskoj and T.Y. Tretyakova, Z. Phys. A **343**, 355 (1992).
 - [36] L.L. Zhang, H.Q. Song, and R.K. Su, J. Phys. G **23**, 557 (1997).
 - [37] H.-J. Schulze, M. Baldo, U. Lombardo, J. Cugnon, and A. Lejeune, Phys. Rev. C **57**, 704 (1998).
 - [38] J. Schaffner and I.N. Mishustin, Phys. Rev. C **53**, 1416 (1996).
 - [39] S. Aoki *et al.*, Prog. Theor. Phys. **85**, 1287 (1991).
 - [40] P. Wang, R.K. Su, H.Q. Song, and L.L. Zhang, Nucl. Phys. **A653**, 166 (1999).
 - [41] D. Halderson, Phys. Rev. C **60**, 064001 (1999).